***New Phytologist* Supporting Information**

Article title: A stomatal control model based on optimization of carbon gain versus hydraulic risk predicts aspen sapling responses to drought
Authors: Martin D. Venturas, John S. Sperry, David M. Love, Ethan H. Frehner, Michael G. Allred, Yujie Wang, and William R. L. Anderegg
Article acceptance date: 08 June 2018

The following Supporting Information is available for this article:

Fig. S1 Experimental design of the research plot.

Fig. S2 Midday weather input variables for the days in which we compare measured vs. modeled output variables running the model from predawn pressures (Objective I).

Fig. S3 Hourly measurements of the main weather inputs required for running the water budget model (Objective II).

Fig. S4 Studentized measured vs. Tuzet model output treatment means.

Fig. S5 Water budget model drought mortality predictive capacity based on whole-plant xylem percent loss in hydraulic conductance.

Fig. S6 Water budget model drought mortality predictive capacity based on whole-plant conductance and xylem conductance.

Methods S1 Modeling canopy sun and shade layers, and evaporation from soil.

Methods S2 Applying the Tuzet model.

Methods S3 Measurement of rock volume in the soil.

Methods S4 A-Ci curve construction.

Notes S1 Model code comments.

Notes S2 Excel file with Visual Basic for Applications macro for initializing K_{max} and % R_l.

Notes S3 Excel file with VBA macro for the gain-risk model running from predawn xylem

pressure.

Notes S4 Excel file with Visual Basic for Applications macro for Tuzet model running from predawn xylem pressure.

Notes S5 Excel file with Visual Basic for Applications macro for the full gain-risk model running from irrigation and rain.

Table S1 Excel file containing the main dataset of this study.

Fig. S1 Experimental design of the plot and photographs from each experimental block (treatment) taken on August 30, 2017. Nine spray sprinklers (Toro 570 Match Precipitation Rate 1.5 m spray nozzles, The Toro Company, Bloomington, MN, USA) provided a homogenous watering pattern.

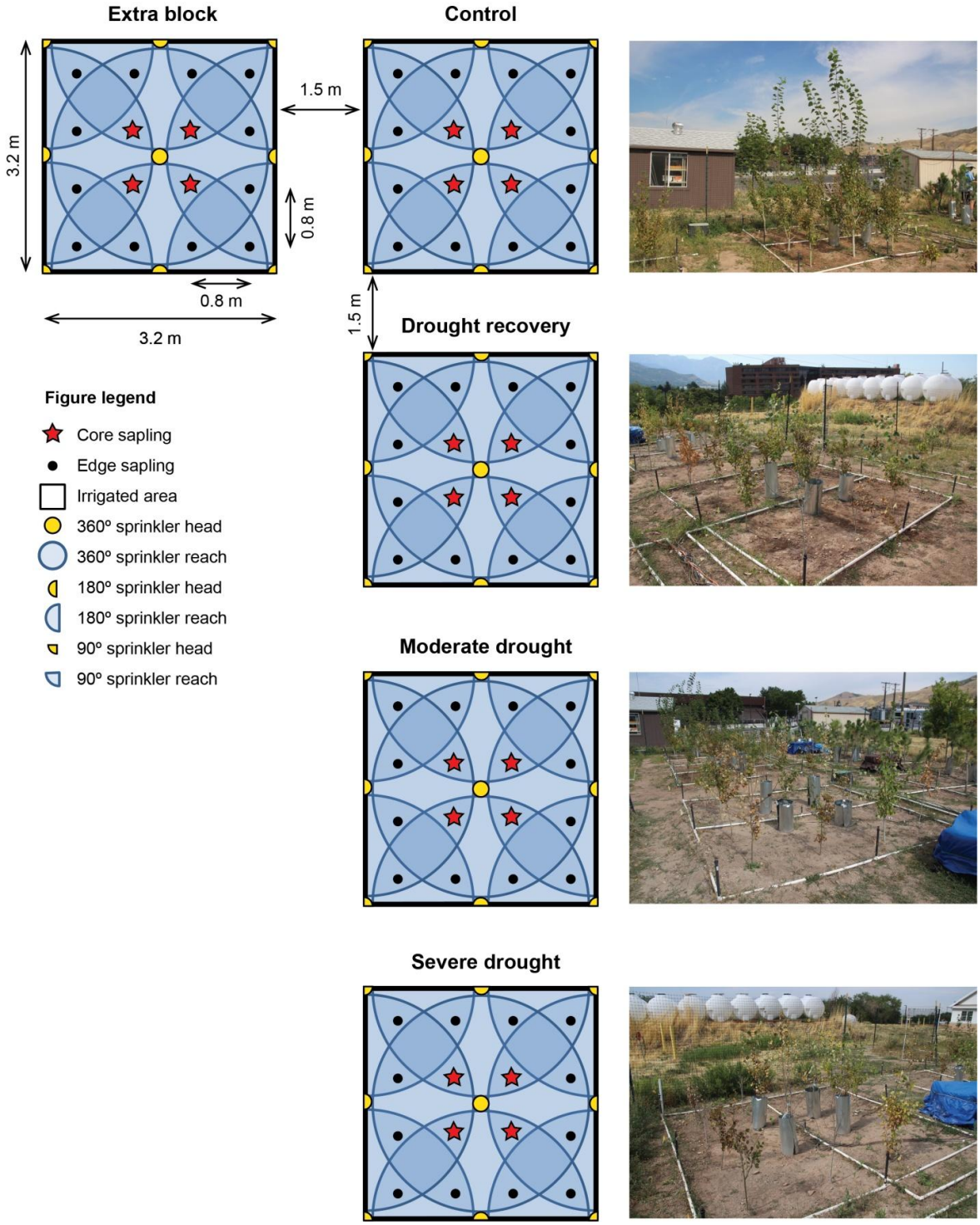

Fig. S2 Midday (11:00 – 12:00 Mountain Standard Time) weather input variables for the days in which we compare measured *versus* modeled output variables running the model from predawn pressures (Objective I). Mean values for solar radiation (W, open circle), wind speed (u, closed circle), air temperature (T_{air}, open square), and air vapor pressure deficit (D_{air}, closed square). The error bars indicate the range (minimum - maximum) within the timestep.

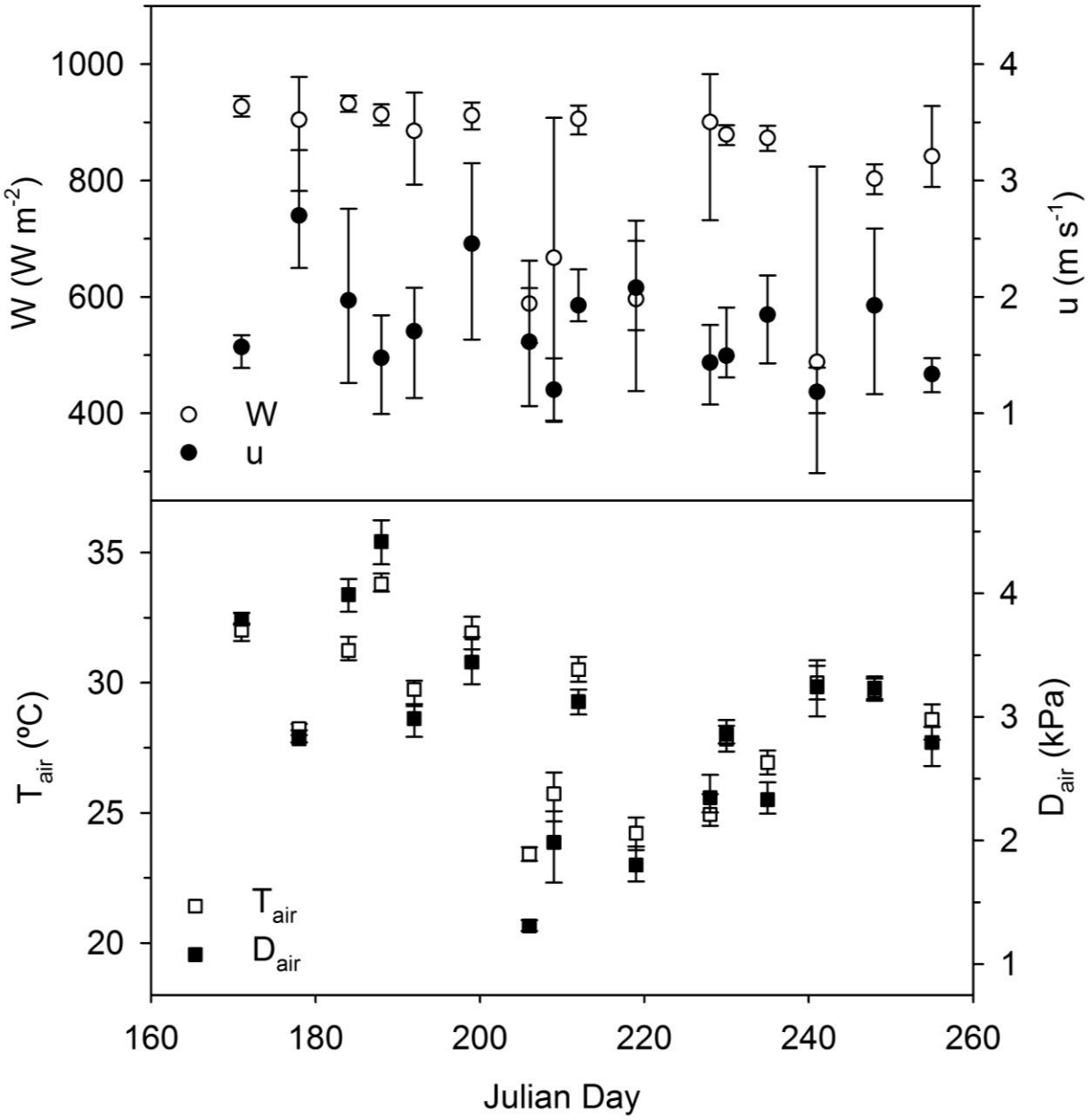

Fig. S3 Hourly measurements of the main weather inputs (air temperature, T_{air}; air vapor pressure deficit, D_{air}; soil temperature, T_{soil}; solar radiation, W; and, wind speed, u) required for running the water budget model.

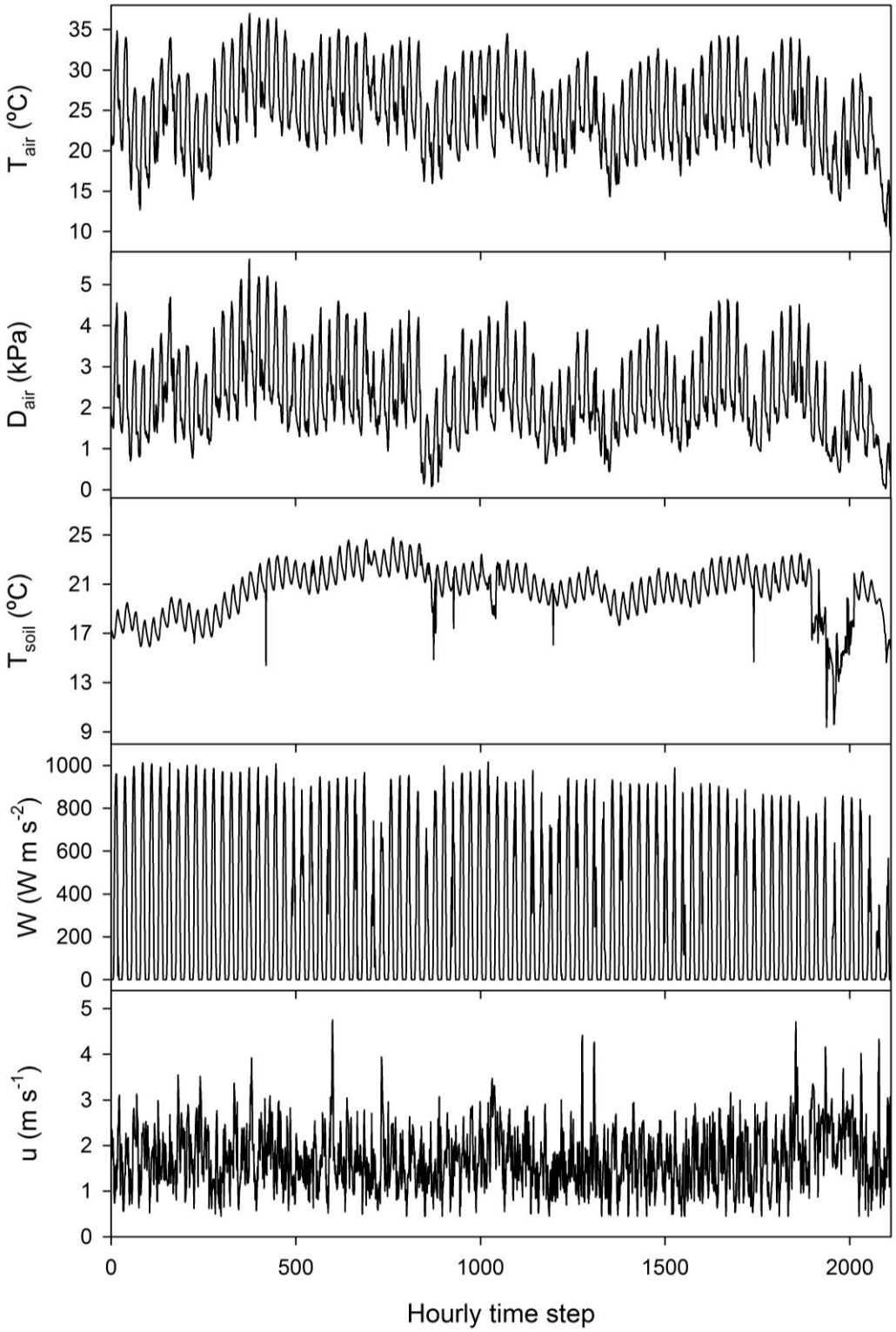

Fig. S4 Studentized measured *vs.* Tuzet model output treatment means. Net assimilation (A_{net}), transpiration (E), diffusive stomatal conductance (G_w), whole-plant hydraulic conductance (K_p), canopy pressure at midday (P_{md}), leaf temperature (T_l), and sap flow (SF) obtained from running the Tuzet model without refilling. Solid black line is the overall regression for the six outputs (n=400, P<0.001, r^2=0.35) and dash-dot line is the 1:1 relationship.

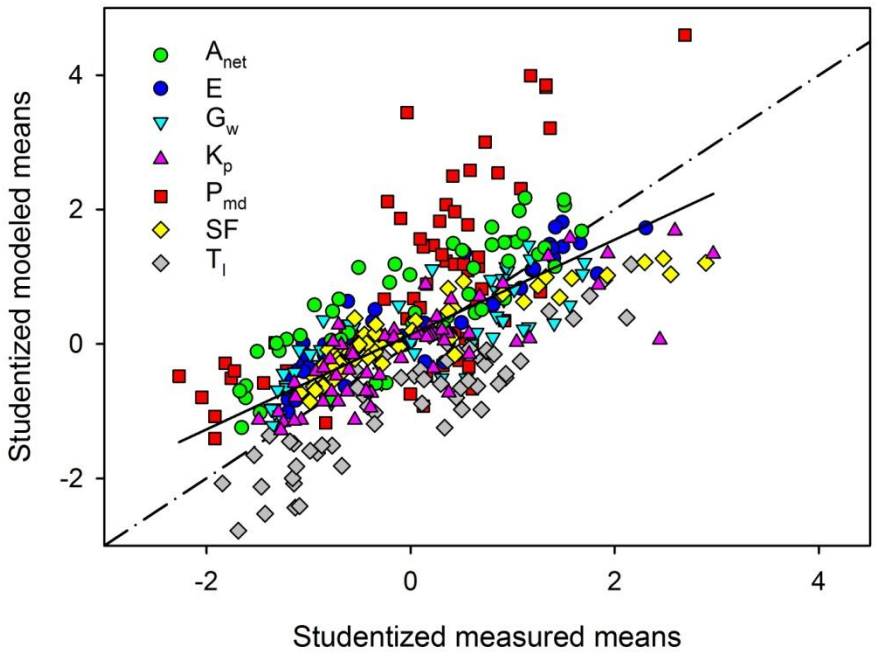

Fig. S5 Water budget model drought mortality predictive capacity based on whole-plant xylem percent loss in hydraulic conductance (PLC_x). **(a)** Modeled PLC_x time course for each of the core saplings (solid lines). Saplings of each treatment are represented with a different color (blue, control; cyan, drought recovery; grey, moderate drought; black, severe drought), and if the tree died the modeled time course is represented in red after tree death. The red dashed line indicates the full-season PLC_x mortality threshold and the magenta dash-dot line the PLC_x threshold at death. Only one sapling of the control treatment is represented since the time course of the four saplings was nearly identical. **(b)** Maximum modeled PLC_x reached by each core tree at time of death (magenta triangles) and at end of the season (red circles), and their logistic death probability regression models (magenta line, at time of death, P = 0.01; red line, at end of season, P < 0.001).

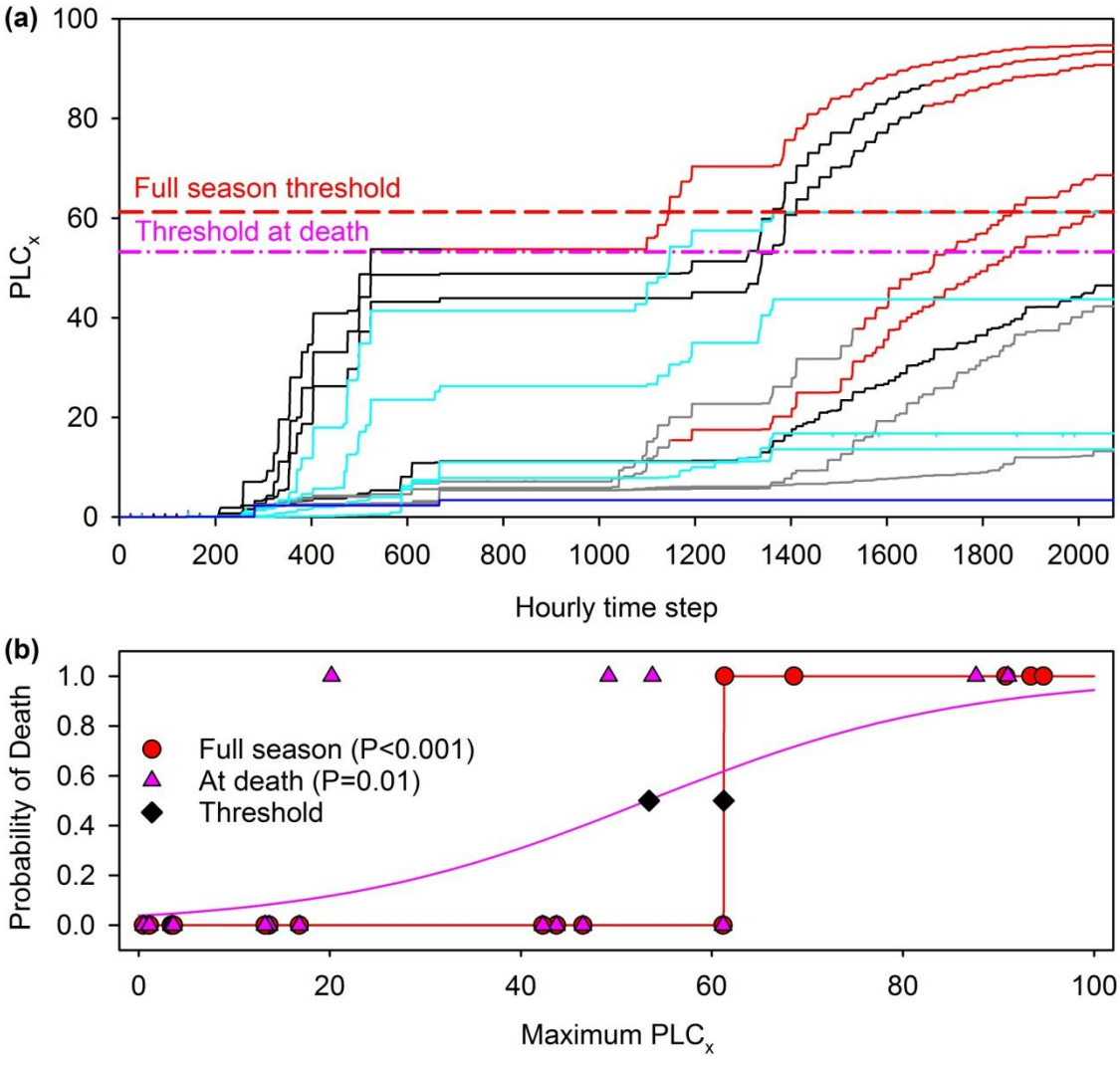

Fig. S6 Water budget model drought mortality predictive capacity based on minimum whole-plant and xylem conductance. **(a)** Minimum whole plant conductance (K_p, per basal area) reached running the model for the full season, **(b)** minimum K_p reached prior to death and for surviving saplings minimum full season K_p, **(c)** minimum whole plant xylem conductance (K_x, per basal area) reached during the full season, and **(d)** minimum K_x reached prior to death and for surviving saplings minimum full season K_x. Grey circles, conductance of the 16 plants; black line, logistic probabilistic regression linking mortality and conductance (P values reported in the panels); white diamond, mortality threshold.

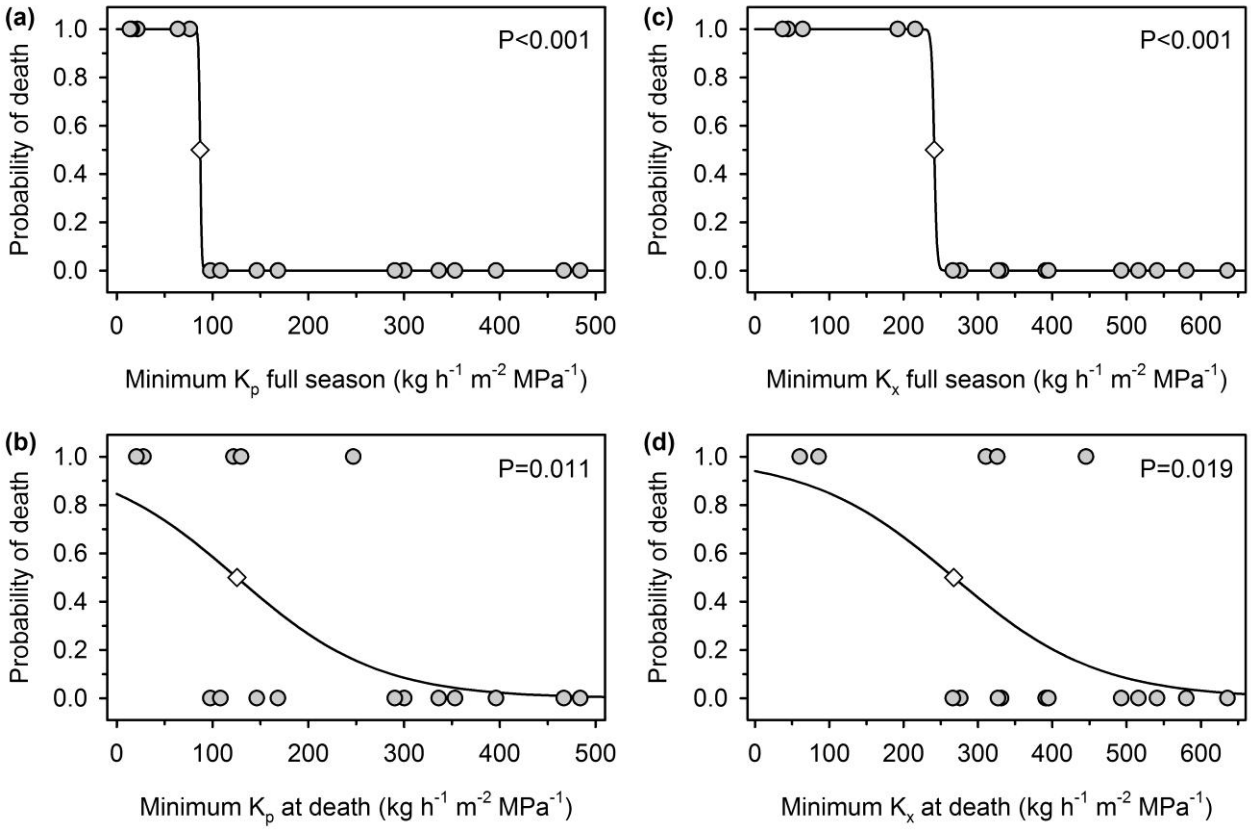

Methods S1 Modeling canopy sun and shade layers, and evaporation from soil.

The division of canopy into sun and shade layers follows the approach detailed in Campbell and Norman (1998). The leaf area index of sun leaves, LAIs, is given by:

$$LAIs = \frac{1-e^{-K_{be}(Y)\cdot LAI}}{K_{be}(Y)} \qquad \text{Eqn. S1,}$$

where LAI is the total leaf area index (from hemispheric photographs), *Y* is the zenith angle of the sun (calculated from time of day, latitude, time of year). The K_{be} is the extinction coefficient of solar beam radiation:

$$K_{be} = \frac{(x^2+tan^2 Y)^{0.5}}{x+1.774\cdot(x+1.182)^{-0.733}} \qquad \text{Eqn. S2,}$$

where *x* is a leaf angle distribution parameter which was assumed 1 for a spherical distribution. Leaf area index for shaded leaves was LAI-LAI_s.

The average photosynthetic photon flux density (PPFD) incident on sunlit leaves, q_s, was

$$q_s = K_{be} \cdot q_b + q_{sh} \qquad \text{Eqn. S3,}$$

where q_b is beam PPFD and q_{sh} is average PPFD (all diffuse) on shaded leaves. The q_b was obtained from calculated clear sky solar radiation (W_c) calibrated (for time of day and clear sky atmospheric transmittance) to match measured solar radiation (*W*) on clear sky days. When *W* ≥ W_c, q_b was calculated from the beam portion of W_c (W_c = diffuse + beam clear sky components). An atmospheric transmittance of 0.4 was used to calculate a W_o threshold for overcast conditions, and q_b = 0 if W ≤ W_o. On partially cloudy days (W_o > *W* < W_c), the beam portion (and hence the estimate of q_b) was assumed to decrease to zero as W decreased to W_o. The remaining diffuse portion of W was converted to PPFD diffuse, q_d, which in turn gave the average estimated diffuse PPFD incident on shaded leaves, q_{ds}:

$$q_{ds} = q_d \cdot \frac{1-e^{-(a^{0.5}\cdot K_d\cdot LAI)}}{a^{0.5}\cdot K_d\cdot LAI} \qquad \text{Eqn. S4.}$$

The *a* is the absorptivity of photosynthetically active radiation for leaves (0.8), and K_d the extinction coefficient for diffuse radiation. The K_d was estimated by integrating Eqn. S2 and corresponding transmittance for *Y* = 0 to 90 degrees as detailed in Campbell and Norman (1998; their Eqn. 15.5). Shade leaves also intercept backscattered PPFD (q_{sc}) from incident beam. The average q_{sc} was estimated as:

$$q_{sc} = \frac{q_{bt} - q_b}{2} \qquad \text{Eqn. S5,}$$

where q_{bt} is direct beam plus backscattered PPFD at the bottom of the canopy, and q_b the beam PPFD at the top of the canopy (see above). The q_{bt} is estimated as:

$$q_{bt} = q_b \cdot e^{-(a^{0.5} \cdot K_{be} \cdot LAI)} \qquad \text{Eqn. S6.}$$

The average PPFD incident on shade leaves (q_{sh}, Eqn. S3) was:

$$q_{sh} = q_{ds} + q_{sc} \qquad \text{Eqn. S7.}$$

The q_s and q_{sh} were used to compute photosynthetic rates and gain functions for sun and shade layers, respectively. An analogous series of equations computed the portion of *W* (photosynthetically active *vs.* near infra-red portions handled separately) reaching sun and shade layers. This, along with long wave radiation, was required as input for computing leaf temperature from leaf energy balance (Campbell & Norman, 1998; Sperry *et al.*, 2017).

Evaporation from bare soil, E_s, was estimated as (Campbell, 1985):

$$E_s = \frac{E_p \cdot (r_{hs} - r_{ha})}{1 - r_{hs}} \qquad \text{Eqn. S8,}$$

where E_p is the potential evaporation rate from a wetted soil surface, r_{hs} is relative humidity at water potential equilibrium with P_s in the top 2 cm soil layer, and r_{ha} is the relative humidity of the air. The E_p was given by:

$$E_p = \frac{R_{abs} - L_{oe} - c_p \cdot (g_r + G_{Ha}) \cdot (T_{soil} - T_{air})}{\lambda} \qquad \text{Eqn. S9,}$$

where R_{abs} is the radiation absorbed by the soil as computed from the canopy light model (soil absorptivity of 0.94 for incoming solar) and long wave emission from the shade layer (0.97 absorptivity for long wave). The long wave emission from soil, L_{oe}, is calculated from measured T_{soil} and an emissivity of 0.97. The specific heat of air is c_p = 29.3 J mol^{-1} C^{-1}. The latent heat of vaporization, λ, and the radiative conductance, g_r, are functions of T_{air} (Campbell & Norman, 1998). The G_{Ha} is the aerodynamic conductance for heat (assumed equal to vapor), and is calculated from the molar density of air (*m*, moles m^{-3}), the understory windspeed (u_s, m s^{-1}), and surface roughness according to Campbell and Norman (1998; Eqn. 7.28):

$$G_{Ha} = \frac{0.16 \cdot m \cdot u_s}{Ln(\frac{z}{z_m}) \cdot Ln(\frac{z}{z_h})} \qquad \text{Eqn. S10,}$$

where *z* is the difference between height of wind-speed estimation and the zero plane displacement for the soil surface (ca. 100 cm), z_m is the momentum roughness length (0.01 cm for a smooth surface), and z_h the heat exchange roughness length (0.002 cm). The u_s at 100 cm was assumed 0.5 times that measured by the onsite weather station.

Methods S2 Applying Tuzet's model.

To find coefficients c_1, c_2 and P_{ref} (Eqn. 8), we maximized the fit between Tuzet model predictions of $\hat{G}_c$, $\hat{A}_{net}$, $\hat{P}_c$ (^ denotes a Tuzet model prediction) *vs.* measured G_c, A_{net}, P_c using the "Solver" routine in Excel. We constrained P_{ref} to be zero or below, but otherwise did not constrain c_1 or c_2. To insure finding a global optimum we started Solver from 100 randomly generated initial values of c_1 (between 10 and 2), c_2 (between 15 and 0), and P_{ref} (between 0 and -3 MPa). Best fit was assessed by minimizing the studentized mean absolute error averaged across predicted *vs.* measured pairs of G_c, A_{net}, and P_c. To studentize, we subtracted the measured mean from each value and divided by the measured standard deviation. Studentizing equalizes the weighting given to error in G_c, A_{net}, and P_c. The Tuzet $\hat{G}_c$ was given by Eqn. 8. Tuzet's $\hat{A}_{net} = \hat{G}_c \cdot C$, where C was the measured CO_2 mole fraction difference between ambient air and the leaf air space. Tuzet's $\hat{P}_c = P_{pd} - \hat{E}/k$, where P_{pd} is the measured predawn xylem pressure and k the measured soil-canopy hydraulic conductance. Tuzet's

$\hat{E} = \hat{G}_w \cdot D_L$, where D_L is the measured H_2O mole fraction difference between saturated leaf air spaces and ambient air. Tuzet's diffusive conductance to water vapor, $\hat{G}_w = \hat{G}_c \cdot (G_w/G_c)$, where G_w/G_c is the measured ratio of diffusive conductance to water vapor *vs.* CO_2.

To apply Tuzet's model, we used the same photosynthetic and hydraulic calculations used by the gain-risk model to calculate the full set of possible values for G_c, A_{net}, P_c (and all other outputs, G_w, E, K, T_l, SF) for each measured P_{pd}. Xylem refilling was turned off. We then found by iteration the one set of values that satisfied Eqn. 8 for the best-fit values of c_1, c_2, and P_{ref}. The Visual Basics Application code is given under Notes S4. The Tuzet values for P_c, E, A_{net}, K, G_w,T_l, SF were compared to measured values to assess model fit (Table 3; Fig. S6).

Methods S3 Measurement of rock volume in the soil.

The rock fraction was estimated by digging a hole and sieving the soil through a 1.2 x 1.2 cm square wire mesh. The hole was lined with a plastic sheeting and its total volume (V_t) was measured from the water required to fill it. The volume of rocks (V_r) was measured by water displacement of rocks larger than the mesh. Rock fraction (V_r/V_t) was averaged over 3 holes.

Methods S4 Construction of A-Ci curves.

For constructing A-Ci curves we performed measurements with an infrared gas analyzer (Licor-6400XT with the 3x2 LED chamber, LI-COR, Lincoln, NE, USA) on one healthy, fully expanded, sun leaf from the top part of the canopy per core tree. Chamber settings were 2,000 µmol photon m^{-2} s^{-1} (i.e., saturating photosynthetically active radiation), T_{air} that gave a $T_l \approx 25$ ºC, and D_{air} between 1.0 and 2.5 kPa. We then sequentially set the chamber CO_2 concentrations at 400, 300, 200, 100, 50, 400, 400, 600, 1,000, 1,500, and 2,000 ppm and recorded measurements once gas exchange stabilized. Measurements were performed between 8:30 and 13:00 MST.

We calculated the maximum carboxylation rate at 25 ºC (V_{max25}) and maximum electron transport rate at 25 ºC (J_{max25}) that provided the best fit by least square means error to internal

CO_2 concentration (C_i) *vs.* net assimilation (A_{net}) measurements. To do so we used the parameters and equations described in Sperry *et al.* (2017; Eqns. 6-8). In short, Rubisco-limited photosynthesis rate (J_c) was calculated as (Medlyn *et al.*, 2002):

$$J_c = \frac{V_{max} \cdot (C_i - \Gamma^*)}{C_i + K_c \cdot \left(1 + \frac{O_a}{K_o}\right)} \quad \text{Eqn. S11,}$$

where V_{max} is the maximum carboxylation rate (µmol CO_2 s^{-1} m^{-2}) at a given leaf temperature, C_i is the internal CO_2 concentration (Pa), Γ* is the CO_2 compensation point (Pa), K_c is Michaelis-Menten carboxylation parameter, K_o is Michaelis-Menten oxygenation parameter, and O_a atmospheric O_2 concentration (Pa). Temperature dependence of these parameters relative to 25 ºC were modeled as (Bernacchi *et al.*, 2001; Leuning, 2002; Medlyn *et al.*, 2002):

$$\Gamma^* = P_{at} \cdot 42.75 \cdot 10^{-6} \cdot e^{\frac{37830 \cdot (T_l - 298)}{298 \cdot R \cdot T_l}} \quad \text{Eqn. S12,}$$

$$K_c = P_{at} \cdot 404.9 \cdot 10^{-6} \cdot e^{\frac{79430 \cdot (T_l - 298)}{298 \cdot R \cdot T_l}} \quad \text{Eqn. S13,}$$

$$K_o = P_{at} \cdot 278.4 \cdot 10^{-3} \cdot e^{\frac{36380 \cdot (T_l - 298)}{298 \cdot R \cdot T_l}} \quad \text{Eqn. S14,}$$

$$V_{max} = \frac{V_{max25} \cdot \left(1 + e^{\frac{-4424}{R \cdot 298}}\right) \cdot e^{\left(\left(\frac{73637}{R \cdot 298}\right) \cdot \left(1 - \frac{298}{T_l}\right)\right)}}{1 + e^{\frac{486 \cdot T_l - 149252}{R \cdot T_l}}} \quad \text{Eqn. S15,}$$

where P_{at} is atmospheric pressure (Pa), *R* the ideal gas constant (8.314 J K^{-1} mol^{-1}), and T_l the leaf temperature (K).

Electron transport-limited photosynthesis (J_e) was calculated as (Medlyn *et al.*, 2002):

$$J_e = \frac{\alpha \cdot Q + J_{max} - \left((\alpha \cdot Q + J_{max})^2 - 4 \cdot c \cdot \alpha \cdot Q \cdot J_{max}\right)^{0.5}}{8 \cdot c} \cdot \frac{(C_i - \Gamma^*)}{(C_i + 2 \cdot \Gamma^*)} \quad \text{Eqn. S16,}$$

where α is the quantum yield of electron transport (0.3 mol photon mol^{-1} electron), *Q* is photosynthetically active radiation (µmol s^{-1} m^{-2}), *c* is the curvature of the light response curve (0.9), and J_{max} is the maximum rate of electron transport (µmol s^{-1} m^{-2}). J_{max} temperature dependence was calculated as (Leuning, 2002):

$$J_{max} = \frac{J_{max25} \cdot \left(1+e^{\frac{-4534}{R \cdot 298}}\right) \cdot e^{\left(\left(\frac{50300}{R \cdot 298}\right) \cdot \left(1-\frac{298}{T_l}\right)\right)}}{1+e^{\frac{495 \cdot T_l - 152044}{R \cdot T_l}}} \quad \text{Eqn. S17.}$$

Gross assimilation rate (A) was calculated as the minimum value of J_c and J_e using a smoothing function (Collatz *et al.*, 1991):

$$A = \frac{J_e + J_c - \left((J_e + J_c)^2 - 4 \cdot c' \cdot J_e \cdot J_c\right)^{0.5}}{2 \cdot c'} \quad \text{Eqn. S18,}$$

where c' is a curvature factor (0.98).

Finally, A_{net} was calculated as:

$$A_{net} = A - R_r \quad \text{Eqn. S19,}$$

where R_r is the respiration rate (µmol s^{-1} m^{-2}) calculated as:

$$R_r = 0.01 \cdot V_{max25} \cdot 2^{\left(\frac{T_l - 298}{10}\right)} \quad \text{Eqn. S20.}$$

Notes S1 Model code comments

Four versions of model code are supplied. Code was written for research purposes only, and no attempt was made to optimize it for public usage. An "instructions" worksheet briefly explains input/output. Notes S2 calculates saturated values of soil-canopy hydraulic conductance (K_{max}) and percentage hydraulic resistance in the leaf (%R_l) from reference values measured in well watered plants (program version: *soil-plant-climate ver 10 INPUT nph.xlsm*). These K_{max} and %R_l values are then inputted to run the model. Notes S3 is the gain-risk model configured to run from predawn xylem pressure (program version: *soil-plant ver 38 generic nph.xlsm*). Notes S4 has the same routines as Notes S3, but configured to calculate Tuzet model output based on Eqn. 8 and coefficients c_1, c_2, and P_{ref} (program version: *soil-plant ver 38 tuzet generic nph.xlsm*). Notes S5 is the gain-risk model configured to run on hourly timesteps, updating the root zone water budget at each timestep (program version: *soil-plant-climate ver 10 generic nph.xlsm*).

References

Bernacchi C, Singsaas E, Pimentel C, Portis Jr A, Long S. 2001. Improved temperature response functions for models of Rubisco-limited photosynthesis. *Plant, Cell & Environment* **24**(2): 253-259.

Campbell GS. 1985. *Soil physics with BASIC: transport models for soil-plant systems*. Amsterdam: Elsevier.

Campbell GS, Norman JN. 1998. *An Introduction to Environmental Biophysics*. New York: Springer.

Collatz GJ, Ball JT, Grivet C, Berry JA. 1991. Physiological and environmental regulation of stomatal conductance, photosynthesis and transpiration: a model that includes a laminar boundary layer. *Agricultural and Forest Meteorology* **54**: 107-136.

Leuning R. 2002. Temperature dependence of two parameters in a photosynthesis model. *Plant, Cell and Environment* **25**: 1205-1210.

Medlyn BE, Dreyer E, Ellsworth DS, Forstreuter M, Harley PC, Kirschbaum MUF, LeRoux X, Montpied P, Strassemeyer J, Walcroft A, et al. 2002. Temperature response of parameters of a biochemically based model of photosynthesis. II. A review of experimental data. *Plant, Cell & Environment* **25**: 1167-1179.

Sperry JS, Venturas MD, Anderegg WR, Mencuccini M, Mackay DS, Wang Y, Love DM. 2017. Predicting stomatal responses to the environment from the optimization of photosynthetic gain and hydraulic cost. *Plant, Cell & Environment* **40**: 816-830.